Determination of Diffusion Coefficients of Metals Dissolved in Mercury by Double Potential Step Chronoamperometry at Hanging Mercury Drop Electrodes

Sang Yun PARK,† Koichi AOKI, Koichi TOKUDA, and Hiroaki MATSUDA*

Department of Electronic Chemistry, Graduate School at Nagatsuta, Tokyo Institute of Technology, Nagatsuta, Midori-ku, Yokahama 227

(Received January 31, 1983)

Double potential step chronoamperometry at the hanging mercury drop electrode is proposed for determination of diffusion coefficients of metals dissolved in mercury. The expression for chronoamperometric curves is obtained, from which the algorithm is derived for evaluating diffusion coefficients of metals. The diffusion coefficients of lead, zinc, and cadmium in mercury at 25 °C were determined by the present technique.

Symbols

- c_O^s Concentration of substance O at the electrode surface.
- c_R^s Concentration of substance R at the electrode surface.
- c_O^* Bulk concentration of substance O.
- D_O Diffusion coefficient of substance O.
- D_R Diffusion coefficient of substance R.
- E_i Initial potential.
- F Faraday constant.
- j_a Anodic current density.
- j_c Cathodic current density.
- n Charge number of the electrode reaction.
- p Intercept of the extrapolated line in the plots of $\phi(\xi)\sqrt{\xi}$ *vs.* $\sqrt{\xi}$.
- q Slope of the extrapolated line in the plots of $\phi(\xi)\sqrt{\xi}$ *vs.* $\sqrt{\xi}$.
- t Electrolysis time.
- r Radius of the hanging mercury drop electrode.
- τ Duration of the first potential step.
- γ Ratio of square root of D_R to that of D_O, defined by Eq. 9.
- ϕ Dimensionless anodic current, defined by Eq. 10.
- θ Dimensionless duration of the first potential step, defined by Eq. 8.
- ξ Dimensionless electrolysis time during the second potential step, defined by Eq. 7.

Electrochemical methods have often been applied to a study on determination of the solubility of metals and the diffusion coefficients of metal atoms in mercury.[1] A classical electrochemical method for determination of the diffusion coefficients of metals in mercury is amalgam polarography developed extensively by Furman and Cooper,[2] Stromberg,[3] and Stackelberg and Toome.[4] This method has difficulties in determining accurately the concentration of dissolved metal, especially when the amalgam is unstable. The other method is linear sweep voltammetry at a hanging mercury drop electrode (HMDE) which was proposed by Stromberg and Zakharova[5] and Baransky[6] and later investigated quantitatively by Tokuda *et al.*[7] This can be undertaken with a simple electrochemical instrument in relatively short time but this method is often subjected to complexity when the charge transfer is slow. A new technique leading to more accurate determination was introduced by Stevens and Shain,[8] which is chronoamperometry following the amalgam formation by a pre-electrolysis at the HMDE. In this method, amalgam is prepared by the long-term electroreduction of the metal ion in solution such that the concentration of metal may be uniform over the whole mercury drop. Stevens and Shain took advantages of characteristics of the spherical diffusion at the HMDE and proposed the method of plotting $It^{1/2}$ against $t^{1/2}$ so that the plots fall into a straight line, where I is the anodic current at electrolysis time, t. Fitak determined the diffusion coefficients of many metals in mercury by this method.[9] However, this method is not necessarily an extensively applicable technique because, during the pre-electrolysis, unstable amalgam may be altered in properties and further the HMDE may be influenced by unexpected fluctuations of temperature and undesirable mechanical vibrations. Therefore it is required to develop a method with a short time window.

We present here a technique of double potential step chronoamperometry at the HMDE, of which conditions are as follows: (a) The HMDE does not contain initially any foreign metal while metal ions are in the solution phase. (b) The potential of the HMDE is initially set at E_i, which is positive enough for no faradaic process to occur. (c) The potential is stepped to a sufficiently negative region corresponding to the limiting diffusion-controlled current for the reduction of the metal ions in the solution, and then switched back to E_i. (d) The duration of the cathodic electrolysis is ranged from a few seconds to some ten seconds and the subsequent anodic current is measured within one second. The equations for the double potential step chronoamperometric curves are derived and the procedures of evaluating the diffusion coefficients of metals in mercury are presented. Furthermore this method is applied to the determination of the diffusion coefficients of lead, zinc and cadmium in mercury.

Theoretical

We consider a simple electrode reaction, $O+ne \rightleftarrows R$, without any chemical complication. We assume that the limiting currents are governed by the spherical diffusion of substance O in the solution and of sub-

† Present address: The Korea Meritime University, 1, Dongsam-Dong, Yongdo-ku, Busan, Korea.

stance R in the mercury drop. This means that the shielding effect of capillary tip and the deviation of the shape of the drop from a perfect sphere are neglected. Further it is assumed that the solution initially contains only the spicies O and supporting electrolytes.

The diffusion equation within the finite spherical region has been solved and the concentrations of O and R at the electrode surface have been expressed as functions of the current density and the electrolysis time.[7]

[A] First Potential Step. Concentrations of the ion and the metal at the surface of the HMDE are given by[7]

$$c_O^s = c_O^* - (\pi D_O)^{-1/2}\int_0^t (j/nF)(t-x)^{-1/2}dx + (1/r)\int_0^t G(D_O(t-x)/r^2)(j/nF)dx, \quad (1)$$

$$c_R^s = (1/r)\int_0^t H(D_R(t-x)/r^2)(j/nF)dx, \quad (2)$$

with

$$G(x) = \exp(x)\,\mathrm{erfc}\sqrt{x} \quad (3)$$

$$H(x) = 1/\sqrt{\pi x} + \exp(x)(1+\mathrm{erf}\sqrt{x}) \quad \text{for } 0<x<0.06, \quad (4)$$

where the function $H(x)$ is the inverse Laplace transform of the asymptotic expansion for $1/(\sqrt{s}\coth\sqrt{s}-1)$. Taking c_O^s to be zero yields the well-known expression for the limiting current density controlled by spherical diffusion,[10]

$$j_c = nFc_O^*\sqrt{D_O}(1/\sqrt{\pi t}+\sqrt{D_O}/r). \quad (5)$$

This equation has been applied to determination of diffusion coefficients of several metal ions with high accuracy in the elaborate operation of the HMDE.[12,13]

[B] Second Potential Step. After the first potential step, of which duration is described as τ, the electrode potential is stepped back to E_i to make the concentration of species R effectively zero at the electrode surface, *i.e.*,

$$c_R^s = 0 \quad \text{for } t>\tau. \quad (6)$$

Substituting condition (6) into Eq. 2 and introducing the dimensionless variable, parameters and function as follows:

$$\xi = D_O(t-\tau)/r^2, \quad (7)$$

$$\theta = D_O\tau/r^2, \quad (8)$$

$$\gamma = (D_R/D_O)^{1/2}, \quad (9)$$

$$\phi(\xi) = -(j_a/nF)[\sqrt{\pi}r/c_O^*D_O], \quad (10)$$

then we have

$$\int_0^\xi H[\gamma^2(\xi-x)]\phi(x)dx = \int_0^\theta H[\gamma^2(\xi+\theta-x)](1/\sqrt{x}+\sqrt{\pi})dx, \quad (11)$$

where j_a is the anodic current density and $\phi(\xi)$ the dimensionless anodic current. Since it is somewhat complicated to solve the above integral equation, details of the derivation are given in Appendix. Then $\phi(\xi)$ is expressed as

$$\begin{aligned}\phi(\xi) = {} & (1+\gamma)[2\exp(\gamma^2\theta)-G(\gamma^2\theta)][1/\gamma\sqrt{\xi}-\sqrt{\pi}\,G(\gamma^2\xi)] \\ & + (2/\sqrt{\pi})[\gamma^2(\xi+\theta)+1]\arctan\sqrt{\xi/\theta} \\ & + 2\gamma(\gamma+1)\sqrt{\theta}\,G(\gamma^2\xi) - 2\gamma(\gamma+1)\sqrt{\xi+\theta} \\ & + (2/\sqrt{\pi})\gamma^2(\gamma+1)\sqrt{\xi\theta}-1/\sqrt{\xi+\theta} \\ & - 1/\gamma\sqrt{\xi}-2(1+\gamma)\gamma^3\int_0^\xi(\xi+\theta-x)^{1/2}G(\gamma^2x)dx. \end{aligned} \quad (12)$$

Equation 12 represents the current-time curve for the second potential step, with the parameters of ξ and θ given by Eqs. 7 and 8, respectively.

In Fig. 1, numerically calculated values of $\phi(\xi)\sqrt{\xi}$, which corresponds to $j_a(t-\tau)^{1/2}$, are plotted against $\sqrt{\xi}$ for $\theta=0.06$ and various values of γ. The integral involved in Eq. 12 was evaluated by Simpson's 1/3 rule. The figure shows that a difference between any two curves increases with a decrease in ξ and that every curve becomes almost a straight line as $\sqrt{\xi}$ tends to zero. Therefore extrapolation of $\phi(\xi)\sqrt{\xi}$ to $\sqrt{\xi}\to 0$ is a useful procedure for determinating D_R. The function, $\phi(\xi)\sqrt{\xi}$, can be expanded about $\sqrt{\xi}=0$, as follows:

$$\phi(\xi)\sqrt{\xi} = p + q\sqrt{\xi} + \cdots, \quad (13)$$

with

$$p = [(1+\gamma)\exp(\gamma^2\theta)(1+\mathrm{erf}(\gamma\sqrt{\theta}))-1]/\gamma, \quad (14)$$

$$q = (4/\sqrt{\pi}-2)\sqrt{\theta}\,\gamma(1+\gamma)-1/\sqrt{\theta}-2(1+\gamma) \times\exp(\gamma^2\theta)[1+\mathrm{erf}(\gamma\sqrt{\theta})]. \quad (15)$$

The parameter p is a main factor for evaluating D_R. If the value of D_O is determined from the cathodic current-time curves during the first potential step by plotting j_c against $t^{-1/2}$ and applying Eq. 5, p and q become experimentally accessible quantities. Since the radius of the HMDE, r, can readily be evaluated, θ becomes a known value. Hence it is possible to obtain γ, that is, D_R, from Eq. 14 in principle. In Fig. 2 theoretical values of p calculated from Eq. 14 are plotted against γ for several values of θ, demonstrating that the slopes of the curves increase with an increase in θ. This indicates that making longer the duration of the first potential step and/or using the HMDE with a smaller radius leads to more accurate determination of the diffusion coefficients.

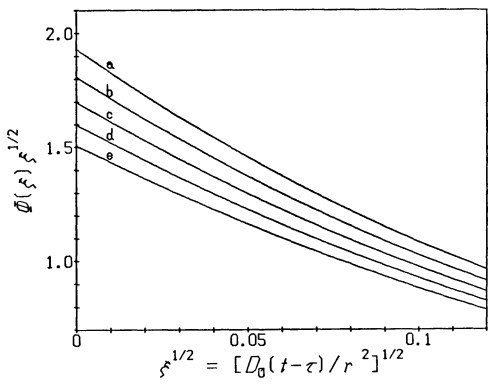

Fig. 1. Variations of $\phi(\xi)\sqrt{\xi}$ with $\sqrt{\xi}$ for $\theta=0.06$ and $\gamma=$(a) : 1.4, (b): 1.2, (c): 1.0, (d): 0.8, (e): 0.6,

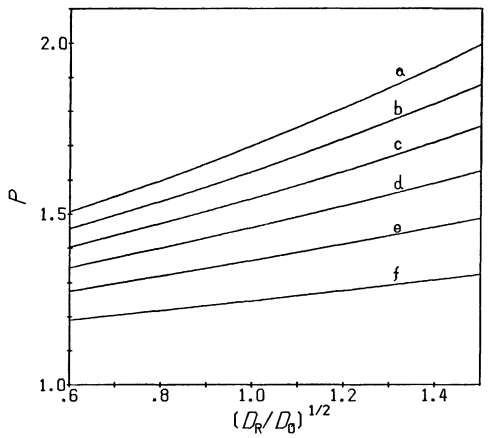

Fig. 2. Dependence of extrapolated values of $\phi(\xi)\sqrt{\xi}$ upon γ for $\theta=$(a): 0.06, (b): 0.05, (c): 0.04, (d): 0.03, (e): 0.02, (f): 0.01.

Since the curves in Fig. 1 have concave forms, extrapolating the curves from the region corresponding to large values of $\sqrt{\xi}$ may yield smaller values of γ than the true ones. We examined the extrapolation procedure of a number of theoretical curves and found that the values of γ can be obtained within 2.5% errors if values of $\sqrt{\xi}$ less than 0.03 are used for extrapolation.

It is not so convenient or elegant to use the working curves in Fig. 2 for evaluating γ from chronoamperometric data. It might be more desirable to utilize the explicit form of γ than to use Fig. 2. Unfortunately, we could not find the inverse function for p. Instead we propose the algorithm for evaluating γ with reasonably high accuracy by Newton-Raphson's method as follows:

$$\gamma_{k+1} = \gamma_k - \frac{[(1+\gamma_k)h_k - 1 - \gamma_k p]\gamma_k}{\left[\begin{array}{l}\{2\gamma_k^2\theta(1+\gamma_k)-1\}h_k \\ \quad +2\sqrt{\theta/\pi}(1+\gamma_k)\gamma_k \exp(-\gamma_k^2\theta)+1\end{array}\right]}, \quad (16)$$

$$h_k = \exp(\gamma_k^2\theta)[1+\mathrm{erf}(\gamma_k\sqrt{\theta})],$$

$(k=0, 1, 2, \cdots)$.

The initial value of γ,γ_0, is usually taken to be unity. Substituting γ_0 and measured value of p into Eq. 16 gives a new value of γ_1, which is again inserted into Eq. 16 to yield γ_2. We confirmed that accuracy with four digits is ensured after two or three iterations.

The values of γ thus evaluated should be consistent with those calculated from slopes of the straight lines by the use of Eq. 15. Since the slope, q, is a secondary term, it is desirable to make use of the slopes for a criterion of the value obtained from p by means of extrapolation. In other words, inserting a value of γ calculated from p into Eq. 15 yields q, which should be the same as that obtained experimentally. If one fails to reach the consistency, the data may be invalid or one can try again to determine γ by varying the slope slightly.

Experimental

Apparatus and Chemicals. A micrometer-type HMDE assembly MCI AS01 (Mitsubishi Chemical Industries, Ltd.) was employed. In order to avoid the shielding of the diffusion space by the capillary wall and to ensure the spherical diffusion as completely as possible, the capillary end was drawn to give a tip of *ca.* 0.2 mm in outer diameter as has been done by Ikeuchi *et al.*[13] Five capillaries were prepared but two of them had good performance in the relation of the size of a mercury sphere to the reading of the micrometer. We paid special attention to the temperature of the cell and mechanical vibrations, to both of which the characteristics of the HMDE are quite sensitive. The H-typed cell with the capillary was dipped into a thermostat at (25± 0.1) °C, which was supported by four semiinflated balls.

All the solutions were made up using Analar grade chemicals and twice-distilled water. Solutions of 3 mmol dm^{-3} of Pb(II) and Cd(II) were prepared by dissolving known amounts of lead oxide and cadmium oxide into solutions of nitric acid, respectively. A supporting electrolyte was sodium sulfate (1.0 mol dm^{-3}).

The electrode potential was controlled with the aid of a home-made potentiostat equipped with a current limiter and a signal generator for clock-controlled potential-time sequences. Transition of the currents was measured with a 12-bit digital oscilloscope (Nicolet 1090A explorer digital oscilloscope).

Procedures. Five glass cups in one centimeter height were placed on the bottom of the cell before passing nitrogen gas through a solution. They function as a vessel for collecting a mercury drop after each experimental run. The initial and the first-step potentials were selected to be about 200 mV more positive and more negative than the half-wave potential, respectively. Durations of the first step used were 3, 7, and 12 s and the current responses were sampled after a 30 ms lapse. Currents during the second potential step were measured in the range from 50 ms to 1 s. Five different radii of the HMDE's were examined. After an experimental run, the HMDE was dropped into one of the glass cups, which was taken out from the cell when five cups were occupied with mercury drops. The mercury drop was rinsed with water, ethanol and acetone in turn and dried. It was weighed immediately after most of acetone was evapolated, because evapolation of mercury causes serious error in determining the radius of a drop. The radius and the area of the HMDE were evaluated from the weight of the drop. Radii of the HMDE were varied from 0.36 mm to 0.55 mm.

Results and Discussion

Plots of the cathodic currents for lead against the reciprocal of the square root of time are shown in Fig. 3. As expected from Eq. 3, the plots fall into a straight line, of which slope gives $nFc_0^*D_0^{1/2}$. The values of D_0 for Pb(II),Cd(II), and Zn(II) ions thus calculated from slopes and Eq. 3 are summarized in Table 1. They were constant regardless of the variations in radii of the HMDE and are quite reasonable values. Unfortunately, we could not find the literature values of D_0 under the same conditions as in this experiment. If we take into account the fact that accuracy of the balance was 0.1 mg, *i.e.*, 4% of relative errors, it turns out that the errors involved in D_0 values can be attributed mainly to errors of weighing mercury drops.

The plots in Fig. 3 deviate upward from the straight line when t $(t<\tau)$ is less than 60 ms. Since we confirmed that the residual cathodic current decays almost

Table 1. Diffusion coefficients of ions in 1 mol dm^{-3} Na_2SO_4 solution and metals in mercury at 25 °C

		$10^{10}D$ / m^2 s^{-1}	Number of runs	Literature values[1] of $10^{10}D$/m^2 s^{-1}
Pb	ion	7.74±0.08(0.50)[a]	33	
	metal	10.5 ±0.26(1.50)	33	11.7
Cd	ion	7.84±0.08(0.29)	12	
	metal	11.4 ±0.2 (0.66)	12	15.2
Zn	ion	7.41±0.08(0.24)	9	
	metal	17.6 ±1.2 (3.00)	6	19.0

a) Digits in the parenthese indicate the standard deviation.

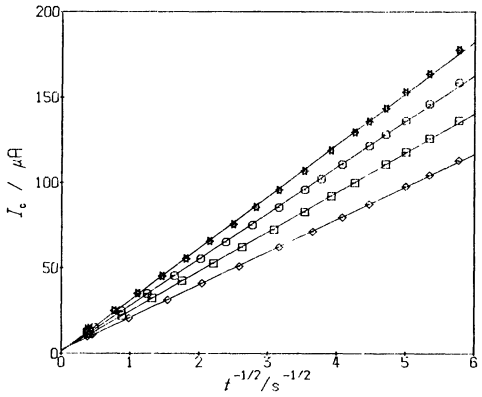

Fig. 3. Plots of cathodic currents *vs.* inverse square roots of time at the HMDE with radii of (★): 0.545, (○): 0.475, (□): 0.445, and (◇): 0.410 mm. The solution was 3 mmol dm^{-3} of Pb^{2+} in 1.0 mol dm^{-3} Na_2SO_4 at 25 °C.

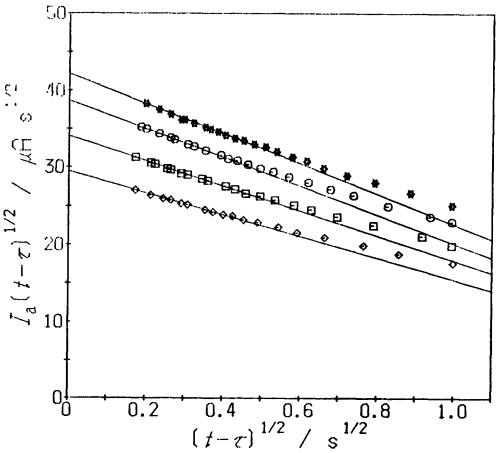

Fig. 4. Plots of products of anodic currents by square roots of time against square roots of time at the HMDE with radii of (★): 0.545, (○): 0.475, (□): 0.445, and (◇): 0.410 mm. The solution was 3 mmol dm^{-3} of Pb^{2+} in 1.0 mol dm^{-3} Na_2SO_4 at 25 °C.

to zero at 4 ms, the deviation cannot be attributed to the charging current. One of the causes of the enhancement of the currents may be the saturation of the potentiostat due to extremely high currents at short times although a current limiter was employed.[13]

The plots of $I_a(t-\tau)^{1/2}$ *vs.* $(t-\tau)^{1/2}$ corresponding to the curves given in Fig. 3 are presented in Fig. 4. The curves in Fig. 4 are quite similar in shape to those of Fig. 1. Since an extrapolated value is required for determination of D_R, it is desirable to measure currents at short electrolysis times. As described above, however, currents obtained at the times less than 60 ms may involve some extraneous components. Plots at the times $(t-\tau)$ more than 0.35 s, which correnspond to $\sqrt{\xi}>0.03$, are ineffective for the extrapolation because of the nature of the concave curves, as predicted from the theoretical curves in Fig. 1. Hence a straight line was drawn for the extrapolation so as to fit the plots in the restricted region (60—350 ms). The procedure for evaluation of D_R is illustrated below by taking the third plot in Fig. 4 as an example. The extrapolated value is 34.0 μA s$^{1/2}$. Substituting this value and the corresponding D_O value ($=7.71\times10^{-10}$ m^2 s^{-1}) into the following equation:

$$p=\lim_{t\to\tau} j_a[\pi(t-\tau)]^{1/2}/nFc_O^*D_O^{1/2}, \quad (17)$$

we obtain $p=1.48$. Since $\tau=7.0$ s, θ is equal to 0.027. Inserting the values of p and θ into Eq. 16, we obtained the recurrent values of γ such as 1.348, 1.326, 1.327, and 1.326, indicating that the convergent value is 1.326. Hence it follows that $D_R=1.02\times10^{-10}$ m^2 s^{-1}. The value of q calculated from Eq. 15 with the values of θ and γ was −12.0, which is in good agreement with the dimensionless slope, −11.6, of the third straight line.

The diffusion coefficients of lead, zinc and cadmium in mercury were determined in this way for some different values of the cathodic pre-electrolysis time, τ, (3—12 s) and the radius of the HMDE, r, (0.36—0.55 mm). The values of D_R obtained are given in Table 1, together with the values suggested by Galus in the light of his present knowledge.[1] These values were constant regardless of variations not only in τ but also in r. We did not observe any dependence of diffusion coefficient of zinc on r although Dowgird and Galus did.[14]

The precision of the values of D_R is twice as poor as that of D_O. The errors may partly result from the extrapolation shown in Fig. 4 and partly be attributed to the double potential perturbation.

Conclusion

The expression for the double potential step chronoamperometric curve has been derived and the procedure for determining the diffusion coefficient of metal in mercury has been developed on the basis of examination of the theoretical curves. The procedure is as follows: (1) D_O is evaluated from the slope of the plots of cathodic currents against $t^{-1/2}$ ($t<\tau$). (2) Anodic currents multiplied by $(t-\tau)^{1/2}$ are plotted against $(t-\tau)^{1/2}$. (3) A part of the straight line of the plots is extrapolated up to $(t-\tau)^{1/2}\to 0$. (4) This extrapolated value and the values of D_O determined in process (1) are inserted into Eq. 16, and the ratio of D_R to D_O is obtained by iterative computation. (5) The slope of the straight line is used for checking whether the extrapolation is reasonable or not.

The measurements for lead, zinc, and cadmium in mercury gave the diffusion coefficients in agreement with literature values. This method is suitable for short time measurement of diffusion coefficients of unstable metals in mercury regardless of the degree of reversibility.

Appendix

The appendix describes details of the derivation of $\phi(\xi)$ from integral equation 11. Applying Laplace transformation with respect to ξ to Eq. 11 yields

$$\begin{aligned}\mathrm{L}[\phi(\xi)]/\gamma(\sqrt{s}-\gamma) &= (s-\gamma^2)^{-1}\\ &\times\int_0^\theta[(\sqrt{s}/\gamma)\exp[s(\theta-x)]\mathrm{erfc}\sqrt{s(\theta-x)}\\ &+\exp[\gamma^2(\theta-x)](1+\mathrm{erf}\sqrt{\gamma^2(\theta-x)})]\\ &\times(1/\sqrt{x}+\sqrt{\pi})\mathrm{d}x, \qquad \text{(A-1)}\end{aligned}$$

where L denotes the operator of the Laplace transformation. The left-hand side has been obtained with the aid of the convolution theorem, whereas the right-hand side has been derived by the direct Laplace integration. Since the integral in Eq. A-1 is of the form of convolution with respect to θ, it is convenient to evaluate the integrals using the convolution theorem for the Laplace transformation. One of the examples is given below.

$$\begin{aligned}&\int_0^\theta\exp[s(\theta-x)]\mathrm{erfc}\sqrt{s(\theta-x)}x^{-1/2}\mathrm{d}x\\ &=\mathrm{L}_\theta^{-1}[\mathrm{L}(1/\sqrt{\theta})\mathrm{L}_\theta(\exp(s\theta)\mathrm{erfc}\sqrt{s\theta})]\\ &=\mathrm{L}_\theta^{-1}[\sqrt{\pi}/u(\sqrt{u}+\sqrt{s})]\\ &=\sqrt{\pi/s}[1-\exp(s\theta)\mathrm{erfc}\sqrt{s\theta}],\end{aligned}$$

where L_θ denotes the Laplace transformation operator with respect to θ and u the Laplace transformed variable of θ. Then the Laplace transformed function of $\phi(\xi)$ becomes

$$\begin{aligned}\mathrm{L}[\phi(\xi)] &= \sqrt{\pi}(1+\gamma)[2\exp(\gamma^2\theta)-G(\gamma^2\theta)]/\gamma(\sqrt{s}+\gamma)\\ &-\sqrt{\pi/s}/\gamma+\sqrt{\pi}G(\theta s)/\gamma\sqrt{s}\\ &-\sqrt{\pi}(1+\gamma)G(\theta s)/\gamma(\sqrt{s}+\gamma). \qquad \text{(A-2)}\end{aligned}$$

Carrying out the inverse Laplace transformation of Eq. A-2 with the help of a table of the transformation[11] yields Eq. 12.

References

1) Z. Galus, *CRC Crit. Rev. Anal. Chem.*, **6**, 359 (1975).
2) N. H. Furman and W. C. Cooper, *J. Am. Chem. Soc.*, **72**, 5647 (1950); W. C. Cooper and N. H. Furman, *J. Am. Chem. Soc.*, **74**, 6183 (1952).
3) A. G. Stromberg, *Dokl. Akad. Nauk SSSR*, **85**, 831 (1952).
4) M. v. Stackelberg and V. Toome, *Z. Elektrochem.*, **58**, 226 (1954).
5) A. G. Stromberg and E. A. Zakharova, *Sov. Electrochem.*, **1**, 922 (1965).
6) A. Baranski, Ph. D. thesis, University of Warsaw, 1974.
7) K. Tokuda, N. Enomoto, H. Matsuda, and N. Koizumi, *J. Electroanal. Chem.*, in press.
8) W. G. Stevens and I. Shain, *J. Phys. Chem.*, **70**, 2276 (1966).
9) S. Fitak, M. Sc. thesis, University of Warsaw, 1973.
10) A. J. Bard and L. R. Faulkner, "Electrochemical Methods: Fundamentals and Applications," John Wiley & Sons, New York (1980), p. 145.
11) G. E. Roberts and H. Kaufman, "Table of Laplace Transforms," W. B. Saunders Company, Philadelphia (1966).
12) H. Ikeuchi, Y. Fujita, K. Iwai, and G. P. Satô, *Bull. Chem. Soc. Jpn.*, **49**, 1883 (1976).
13) H. Ikeuchi, K. Iwai, M. Kaneko, M. Maya, and G. P. Satô, *Bull. Chem. Soc. Jpn.*, **52**, 1863 (1979).
14) A. Dowgird and Z. Galus, *Bull. Acad. Pol. Sci., Ser. Sci. Chim.*, **18**, 225 (1970).